



The impact of COVID-19 public health restrictions on particulate matter pollution measured by a validated low-cost sensor network in Oxford, UK

Tony Bush^{a,b}, Suzanne Bartington^c, Francis D. Pope^d, Ajit Singh^{c,d}, G. Neil Thomas^c, Brian Stacey^e, George Economides^f, Ruth Anderson^f, Stuart Cole^f, Pedro Abreu^g, Felix C.P. Leach^{a,*}

^a Department of Engineering Science, University of Oxford, Parks Road, Oxford, OX1 3PJ, UK

^b Apertum Consulting, Harwell, Oxfordshire, UK

^c Institute of Applied Health Research, University of Birmingham, Edgbaston, Birmingham, B15 2TT, UK

^d School of Geography, Earth and Environmental Sciences, University of Birmingham, Edgbaston, Birmingham, B15 2TT, UK

^e Ricardo Energy and Environment, The Gemini Building, Fermi Avenue, Harwell, Didcot, OX11 0QR, UK

^f Oxfordshire County Council, County Hall, New Road, Oxford, OX1 1ND, UK

^g Oxford City Council, Town Hall, St Aldate's, Oxford, OX1 1BX, UK

ARTICLE INFO

Original content: https://deposit.ora.ox.ac.uk/concern/datasets/uuid_3ea5302b-c151-4c35-a4b7-0269c36fd9c?locale=en

Keywords:

Particulate matter
PM₁₀
PM_{2.5}
Pollution
Traffic
Public health restrictions
Low-cost sensor

ABSTRACT

Emergency responses to the COVID-19 pandemic led to major changes in travel behaviours and economic activities with arising impacts upon urban air quality. To date, these air quality changes associated with lockdown measures have typically been assessed using limited city-level regulatory monitoring data, however, low-cost air quality sensors provide capabilities to assess changes across multiple locations at higher spatial-temporal resolution, thereby generating insights relevant for future air quality interventions. The aim of this study was to utilise high-spatial resolution air quality information utilising data arising from a validated (using a random forest field calibration) network of 15 low-cost air quality sensors within Oxford, UK to monitor the impacts of multiple COVID-19 public health restrictions upon particulate matter concentrations (PM₁₀, PM_{2.5}) from January 2020 to September 2021. Measurements of PM₁₀ and PM_{2.5} particle size fractions both within and between site locations are compared to a pre-pandemic related public health restrictions baseline. While average peak concentrations of PM₁₀ and PM_{2.5} were reduced by 9–10 µg/m³ below typical peak levels experienced in recent years, mean daily PM₁₀ and PM_{2.5} concentrations were only ~1 µg/m³ lower and there was marked temporal (as restrictions were added and removed) and spatial variability (across the 15-sensor network) in these observations. Across the 15-sensor network we observed a small local impact from traffic related emission sources upon particle concentrations near traffic-oriented sensors with higher average and peak concentrations as well as greater dynamic range, compared to more intermediate and background orientated sensor locations. The greater dynamic range in concentrations is indicative of exposure to more variable emission sources, such as road transport emissions. Our findings highlight the great potential for low-cost sensor technology to identify highly localised changes in pollutant concentrations as a consequence of changes in behaviour (in this case influenced by COVID-19 restrictions), generating insights into non-traffic contributions to PM emissions in this setting. It is evident that additional non-traffic related measures would be required in Oxford to reduce the PM₁₀ and PM_{2.5} levels to within WHO health-based guidelines and to achieve compliance with PM_{2.5} targets developed under the Environment Act 2021.

1. Introduction

Ambient air pollution is a major global environmental and health concern which exerts direct and indirect health, environmental and

economic costs upon urban areas in the UK [1]. Exposure to Particulate Matter (PM) is particularly harmful for human health with consistent epidemiological evidence for an association with increased risk of acute and chronic diseases including asthma, coronary heart disease, stroke,

* Corresponding author.

E-mail address: felix.leach@eng.ox.ac.uk (F.C.P. Leach).

<https://doi.org/10.1016/j.buildenv.2023.110330>

Received 12 October 2022; Received in revised form 14 April 2023; Accepted 17 April 2023

Available online 21 April 2023

0360-1323/© 2023 The Authors. Published by Elsevier Ltd. This is an open access article under the CC BY license (<http://creativecommons.org/licenses/by/4.0/>).

lung cancer and all-cause mortality [2–4]. In addition to the impacts on physical health, there is a growing body of literature linking PM air pollution to adverse cognitive and mental health outcomes [5,6]. Recent evidence suggests that there are health benefits to be gained from reductions in PM to levels lower than the existing UK regulatory thresholds and this is reflected in WHO 2021 Global Air Quality Guidelines [7, 8].

The coronavirus disease (COVID-19) caused by Severe Acute Respiratory Syndrome Coronavirus 2 (SARS-CoV-2) led to a global pandemic with major economic and societal consequences. Following the declaration of a global pandemic on 11 March 2020 [9], successive countries rapidly adopted emergency public health measures including social distancing, amenity closures and travel restrictions. These measures in turn led to unprecedented changes in industrial, commercial, and societal activity and behaviours. Reduced transport activity, for example, has been linked by studies across the globe to major reduction in ground level primary air pollutant emissions and ambient NO_2 concentrations [10–12]. Direct before and after comparisons undertaken at city or regional levels can be misleading, given the influences of seasonal trends, meteorological conditions, and urban form upon local pollutant concentrations within densely populated city settings [13]. In addition, the influence upon PM concentrations of primary and secondary contributions and a wider range of emissions sources, further decouple ambient PM levels from changes in transport-related emissions, with evidence for minimal changes in many cities. Application of machine learning approaches to account for changes in weather and seasonal trends have suggested actual increases in PM concentrations during lockdown periods in London [14] and Oxford [15]. However, few studies have considered impacts of lockdown measures on air quality when using sensors at multiple city locations, enabling insights to be generated regarding the spatial impacts of a range of lockdown measures upon real-time particulate pollutant concentrations [16].

Low-cost air quality sensors, offer utility to enhance the spatial coverage relative to high-quality (regulatory grade) measurements which have historically been domain of expensive monitoring equipment [17]. In this context, low-cost sensors might be ones that cost of order low thousands of dollars, rather than regulatory grade equipment which would cost of order high-tens or even hundreds of thousands of dollars. Cheaper sensors, to the order of several hundred dollars, are available, but these typically might not have the durability (and power) to be deployed in the field unattended for years [18,19]. Sensor technologies provide options for capturing the impacts of air quality interventions and hot-spot assessment [20], providing flexibility, minimal infrastructure needs and, therefore suitability for evaluating spatio-temporal variability in pollutant levels [21–23]. In this work fixed, permanently powered, sensors are used, but technology has advanced such that alternatives such as wearable sensors are also available [24]. In addition, advances in sensor technology offer potential for supplementing regulatory monitoring, modelling and the source attribution evidence base for a better-informed exposure estimates and policy decisions [25–27]. This is particularly important for future data capture given the Environment Act Population Exposure Reduction target for $\text{PM}_{2.5}$ concentrations (a reduction in $\text{PM}_{2.5}$ population exposure of 35% compared to 2018 to be achieved by 2040), alongside revised UK Air Quality Objectives [28]. Few studies have utilised low-cost sensor technology to assess impacts of COVID-19 in urban areas and to the best of the authors' knowledge none have been undertaken in medium-sized cities such as Oxford [29,30].

This study investigates changes in PM (PM_{10} and $\text{PM}_{2.5}$) concentrations for successive phases of COVID-19-related restrictions using high-spatial resolution data generated by a validated low-cost sensor network in Oxford, UK. The validation is achieved using a Random Forest Machine Learning technique for field calibration, achieving high levels of confidence in the data developed in the authors' previous work [31]. Comparison of changes in PM occurring at multiple locations in this real world natural experimental study will inform prospective city-level air

quality interventions and therefore present opportunities to benefit human health.

2. Methodology

2.1. Study setting

Oxford is a dynamic international city, with a population of 152,450 residents (ONS 2019 mid-year estimate) and 32,930 students enrolled at two universities [32]. At least 46,000 people commute into the city for work on a daily basis [33]. Oxford has recognised challenges of poor air quality and in 2010, the whole city was declared an Air Quality Management Area (AQMA) [34]. Subsequently in 2014, a central Low Emission Zone (LEZ), focussing on bus emissions [20], was introduced and then further extended in 2020 [34]. In 2021, the city council formally committed to a set of policy actions outlined in its revised Air Quality Action Plan [34], with the introduction of a central 'Zero Emission Zone' in February 2022 [35].

Long-term trends in PM levels in Oxford have been characterised from measurements at two locations; Oxford High Street, a roadside location locally operated by Oxford City Council and Oxford St Ebbe's (UKA00518), an Automated Urban and Rural Network (AURN) urban background location. In 2019, the annual mean $\text{PM}_{2.5}$ concentration was $9 \mu\text{g}/\text{m}^3$ at the urban background which exceeds the 2021 WHO Global Air Quality Guideline recommendation of $5 \mu\text{g}/\text{m}^3$ [34] but is within the UK Air Quality Objective of $10 \mu\text{g}/\text{m}^3$ [36]. To date, few policy measures have been adopted within Oxford to specifically address PM emissions, which have reduced only marginally in recent years. To illustrate, Fig. 1 presents monthly mean PM concentrations at roadside and urban background for the period 2014–2021; the trend in each is shown by an ordinary least squares (OLS) regression line. Fig. 1 shows that the rate of decline in PM levels is around 25% over 8 years and similar at both urban background and roadside. Considering the local policy efforts to reduce road transport emissions over this period, such as the AQMA, LEZ, and ZEZ, this slow rate of decline is indicative of other, important non-road transport sources of PM influencing local concentrations. Source apportionment studies in Oxford have estimated that road transport accounts for $\sim 10.4\%$ PM_{10} emissions and 9.8% of $\text{PM}_{2.5}$ emissions respectively, with domestic combustion being the largest source [34]. Natural PM make up less than 9% for both PM_{10} and $\text{PM}_{2.5}$.

2.2. Calculation of baseline particle concentrations

Baseline pre-pandemic PM levels were established using hourly measured data between 2016 and 2019 from the St Ebbe's urban background reference instrumentation. Fig. 1 showed that trends in both PM_{10} and $\text{PM}_{2.5}$ in recent years were broadly similar, making this a suitable baseline for pre-pandemic PM.

Using this baseline dataset at a 1-h time resolution, the daily mean and an estimate of daily peak concentrations were derived for both PM_{10} and $\text{PM}_{2.5}$. The daily mean metric is recommended as a short-term guide level for PM [8], and in legally binding objectives [37] and limit value [38]. Peak concentrations were defined as the 95th percentile of daily 1-h concentrations as this excludes outliers from the sensor datasets which are known to occur and coincided with periods of intense local emissions activity (e.g. rush hour) and periods of higher domestic fuel use (e.g. morning/evening). It was hypothesised that lockdown events may affect peak concentrations arising from some of these sources, particularly rush hour events due to a substantial reduction in traffic.

Daily mean and peak PM_{10} and $\text{PM}_{2.5}$ concentrations were calculated daily for the calendar years of 2016–19 and subsequently averaged for each ordinal calendar day to provide a daily marker of pre-pandemic concentrations for each metric in recent years. Fig. 2 presents a time series of the pre-pandemic daily mean PM_{10} and $\text{PM}_{2.5}$ concentrations and Fig. 3 pre-pandemic peak concentrations (95th percentile of daily 1-h mean concentrations) with both displaying large day-to-day variation

throughout the year and some degree of seasonality. This variability limits their utility as an indicator of pre-pandemic mean and peak PM values for comparison with those observed during COVID-19 restriction events. To improve this as a marker for pre-pandemic concentrations, a monthly (28-day) rolling mean was therefore calculated (orange lines). The rolling average technique both reduced the day-to-day variation and minimised the lag artefact commonly found with standard moving/rolling average techniques and facilitates the comparisons of daily pre-pandemic baseline vs. daily concentrations during COVID-19 restriction events.

2.3. Calculation of changes in particle concentrations during COVID-19 restriction periods

Differences in the levels of PM₁₀ and PM_{2.5} measured during COVID-19 restriction events compared to the pre-pandemic baseline (on equivalent ordinal days) were used to evaluate the impact of COVID-19 restrictions, whilst accounting for seasonal trends. The statistical significance of deviations identified was tested using a non-parametric Wilcoxon signed test [39]. A non-parametric test was chosen because air quality datasets do not generally conform to a normal distribution and, in addition, the sample size of the datasets being tested were small when disaggregated to a COVID-19 lockdown event level, see Table 1.

2.3.1. COVID-19 restriction events

Eleven key COVID-19 emergency restriction events occurring during

the study period were identified (Table 1). The events chosen were those expected to have greatest impact upon local air quality. Events lasting less than 10 days long were aggregated into groups of longer duration. Event details, including start/end dates were obtained from official national and local sources [40–42].

Despite the definitive dates presented in Table 1, the effect of advanced warning of events (from government authorities) upon the behaviour of residents is noteworthy, particularly in the transition from one lockdown state to the next. This is illustrated in Fig. 4, which shows the traffic levels on the High Street in central Oxford throughout the period of the study. It is clear that following escalation of the national alert level, and increasing media attention, prior to the introduction of the first national lockdown (event ‘b’ in Table 1), the traffic levels reduce sharply as residents made changes in travel behaviours even before the official enforcement date of 23 March 2020.

2.4. Particle sensors

A network of Praxis Urban sensor systems supplied by South Coast Science Ltd was used in this work [43]. This sensor platform was equipped with an Alphasense N3 optical particle counter (OPC) [44]. This sensor was chosen for a variety of reasons, firstly, the unit cost of the OPC-N3 is relatively low (~£250) when compared to reference grade OPC instruments. Secondly, it is currently the low-cost OPC sensor with the most independent testing and validation in the scientific literature [31,45]. Thirdly, access to raw sensor information (voltages) available

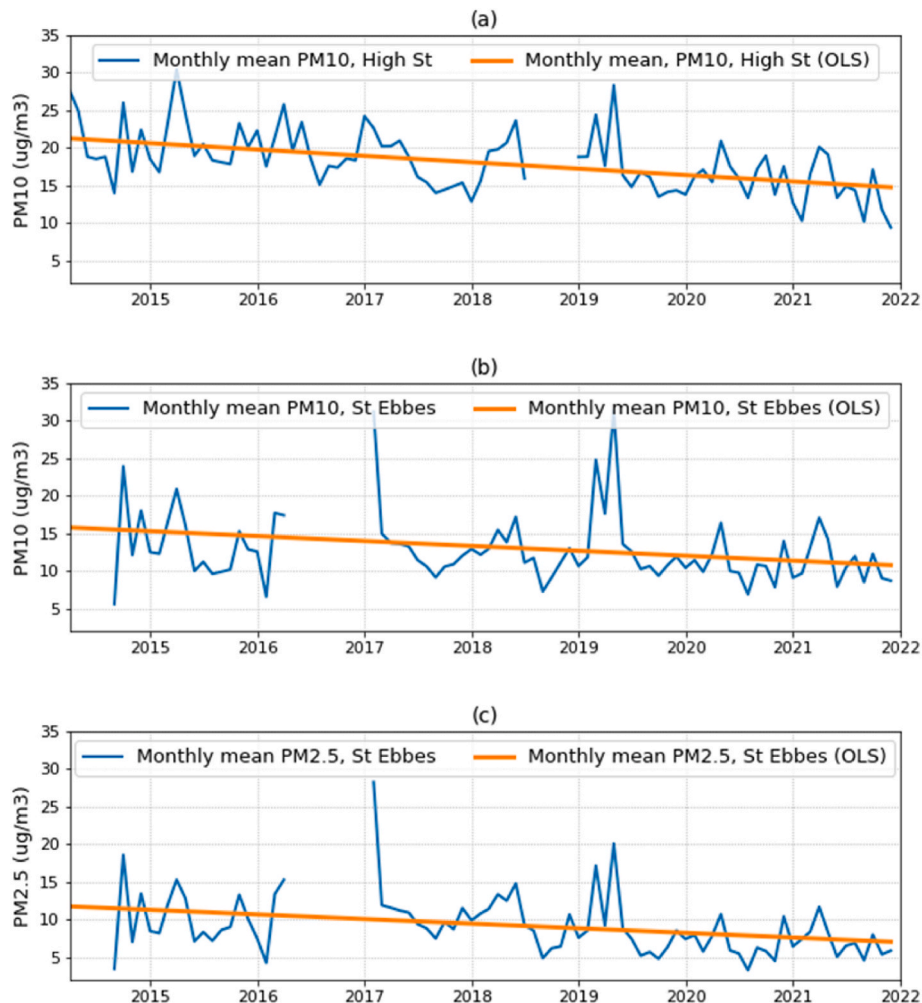


Fig. 1. Monthly mean PM₁₀ and PM_{2.5} concentrations and the OLS trend line at two locations in Oxford 2014–2021. (a) PM₁₀ High St, (b) PM₁₀ St Ebbe's, (c) PM_{2.5} St Ebbe's.

remotely enables high-fidelity, independent data analysis and data quality assurance processes to be undertaken. This counter categorises the sensed particles into ‘bins’ of particle size based on the extent of laser light scattering to derive a mass fraction of PM_{10} and $PM_{2.5}$ [26,43,44]. The sample logging rate of the OPC sensor was set to 10 s intervals (0.1 Hz). Data were then aggregated to a 15-min mean for comparison with the reference measurements and 1-h mean for comparison with baseline measurements. Sensor data were aggregated to a 15-min mean resolution, from the initial logging interval of 10 s, to ensure conformity with the time datum for the AURN datasets.

2.5. Reference measurements

To assess the performance of the Praxis sensors, reference measurements of ambient PM_{10} and $PM_{2.5}$ were obtained from the Defra, Oxford St Ebbe’s AURN monitoring station (UKA00518) [46] and the Oxford City Council managed Oxford High Street monitoring station [47]. Oxford St Ebbe’s employs a Palas Fidas 200 fine dust aerosol optical spectrometer [48]. The Fidas method is a designated, type approved reference instrument for regulatory compliance monitoring [49]. The Oxford High Street monitoring station employs a TEOM 1400 fine dust mass measurement unit with an 8500 Filter Dynamics Measurement System (FDMS) fitted. The FDMS method is a designated as equivalent to the reference method [50]. Reference measurements were obtained at 15-min average resolution by special arrangement with the network operators for the period 1st January 2020 to 18th October 2021. The quality assurance status of the AURN datasets was valid/verified. Sensor and reference method sample inlets were co-located within 2 m for the study duration and at the same height.

2.6. Sensor locations

The Praxis sensors were deployed at 15 locations around Oxford from January 2020 onwards. Deployment at some sites was delayed by the onset of the public health restrictions associated with the pandemic, but the full network was operational from August 2020. A map of Praxis sensor locations and the pre-existing regulatory reference measurement location is shown in Fig. 5.

Sensor based air quality monitoring continued uninterrupted until September 2021 at the 15 locations listed in Table 2. Two sensors were co-located with the regulatory grade reference instrumentation. A list of sensor location names and environment types is presented in Table 2.

Environment type attribute describes the classification of the sensor location using the nomenclature used in the UK [51]. The nomenclature was extended for this work to include an ‘urban intermediate’ classification for sensor locations which did not strictly conform to either ‘urban traffic’ nor ‘urban background’ classifications e.g. were >12 m from the side of a road with significant traffic but remained likely to be influenced by emissions from that adjacent road.

2.7. Field calibration of sensors using a random forest model

Sensor data were calibrated using an extension to the techniques previously described by Bush et al. [31] which proposed a simple and flexible machine learning (ML) method to attenuate for sensor baseline offset and multiple environmental interferences acting upon an OPC sensor signal. The method incorporates a combination of re-weighted regression (adaptive iteratively reweighted Penalized Least Squares - AIRPLS) [52] and a random forest (RF) regression [53] to limit, respectively, sensor offset and environmental interferences (including other sensor characteristics such as sample flow rate and raw electrode voltage readings). The method has been proven to deliver good results when trained with reference data at an urban background location with coefficient of determination values for the relationship between corrected sensor and reference method of 0.79 (PM_{10}) and 0.91 ($PM_{2.5}$) using the ML validation dataset.

2.7.1. RF correction model optimisation

To optimise the method previously presented by Bush et al., for application under the conditions experienced in this study, sensitivity tests were conducted on the RF correction model. These informed the best configuration of the model for field calibration. Model re-training was conducted on 60% of the co-located sensor compared to reference method sample population available for this study. The performance of the model was then tested/validated on the remaining 40% with both samples selected at random. The sensitivity tests showed that:

1. To achieve satisfactory levels of uncertainty in the corrected dataset, model training using the full sample population of the study was required, March 2020 to September 2021. Training and validating over shorter periods resulted in unsatisfactory model performance on unseen proportions of the time series (as has been seen in other work, such as deSouza et al. [54]).

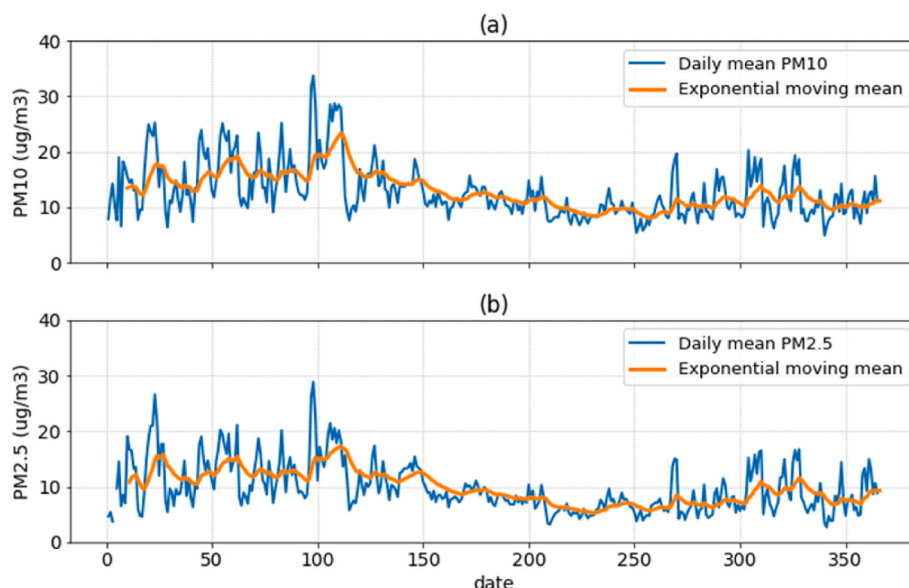


Fig. 2. Average daily mean and associated moving average of daily mean PM_{10} and $PM_{2.5}$ concentrations, St Ebbe’s 2016–2019. (a) PM_{10} , (b) $PM_{2.5}$.

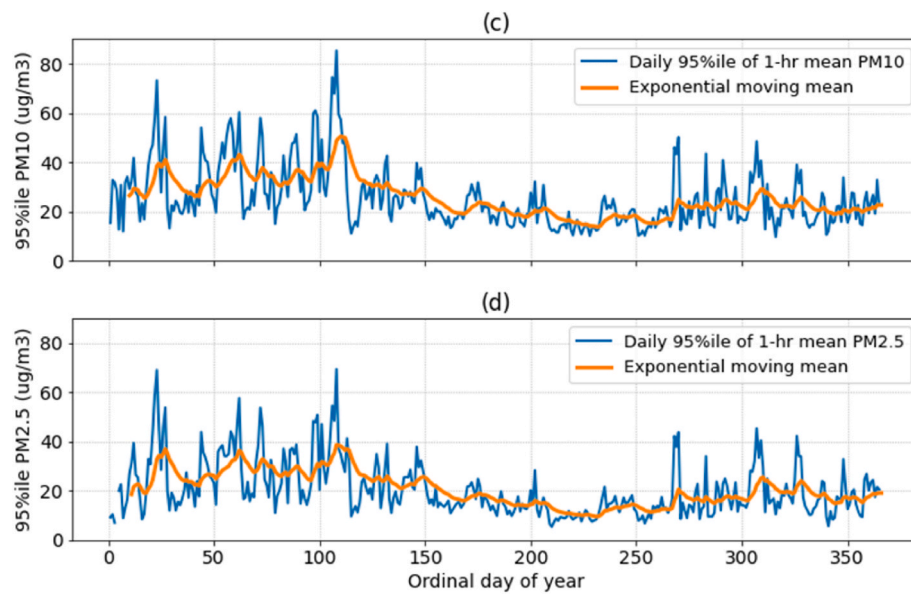


Fig. 3. Average daily 95th percentile of 1-h PM₁₀ and PM_{2.5} concentrations and associated moving average measured, St Ebbe's 2016–2019. (a) PM₁₀, (b) PM_{2.5}.

Table 1

UK and Oxfordshire COVID-19 lockdown transition descriptors and dates (inclusive).

Event code	Title	Description	Start date	End date	Event length (days)
a	Pre-lockdown	Business as usual	2020-01-01	2020-03-22	82
b	National lockdown	First national lockdown	2020-03-23	2020-06-15	48
c	Gradual lifting of restrictions	Schools & retail opens	2020-06-16	2020-09-24	137
d	Tiered restrictions	Medium to high alert local measures	2020-09-25	2020-11-04	42
e	National lockdown	Second national lockdown	2020-11-05	2020-12-01	27
f	Tiered restrictions	Stay at home & high alert local measures	2020-12-02	2021-01-04	34
g	National lockdown	Third national lockdown	2021-01-05	2021-03-07	62
h	Step-1 out of lockdown	Stay at home lifted, schools re-open	2021-03-08	2021-04-11	35
i	Step-2 out of lockdown	Non-essential retail re-opens	2021-04-12	2021-05-16	35
j	Step-3 out of lockdown	Gathering <30 people permitted outside	2021-05-17	2021-06-20	35
k	Step-4 out of lockdown	Most restrictions lifted	2021-06-21	–	–

2. Further model performance benefits could be achieved by the inclusion of paired sensor-reference method data from data from both High St and St Ebbe's monitoring locations. The inclusion of data from traffic orientated High St location complemented that provided by the urban background St Ebbe's location and promoted diversity in the training and validation set.

The behaviours noted above were likely driven by the short temporal duration of the datasets available for model training and the limited diversity found in these data. This attribute of the sample population had potential to detracted from study aims regarding characterisation of conditions during restriction events. As a result, this limitation was

mitigated against using the methods outlined noted above. RF modelling was performed in Python using the scikit-learn open-source machine learning library [55]. Full details of the development of the RF regressor models including optimised hyperparameter settings and feature selection are described by Bush et al. Table 3 presents a summary of the hyperparameter settings for the scikit-learn RF regressor model implementation (using the squared error function to measure the quality of a split). All other model parameters were set to default settings. The maximum number of leaf nodes hyperparameters used for this study were established using a cross-validation sensitivity test also described in detail in Bush et al.

2.7.2. RF correction model validation

Validation outputs from optimised correction models are shown in Fig. 6 for PM₁₀ and PM_{2.5} respectively, based on 1-h averaged data. At this time resolution, the correction models deliver datasets with a coefficient of determination (R^2) of 0.90 for PM₁₀ and 0.95 for PM_{2.5}. The improvement in the performance of the sensors following the RF correction model is large. Table 4 shows the performance of the RF corrected data to simple baseline corrected data. More details in the method behind this are given in previous work by the authors [31].

2.7.3. Expanded uncertainty calculations

Previous work [31] has shown that the expanded uncertainty estimates for corrected sensor datasets, exceeded the levels required of indicative measurements and supplementary assessment techniques for PM (expanded uncertainty < $\pm 50\%$), as set out by the European ambient air quality Directives [38].

As a final step in the model optimisation exercise the expanded uncertainty of corrected datasets were calculated using the spreadsheet tool mandated by the CEN working group [56]. In these calculations, corrections to compensate for non-unity slope and intercept terms within the OLS regression equation are also permitted. Fig. 4a and b presents outputs from these calculations for the final corrected sensor data vs paired reference values. For PM₁₀, the R^2 value for final corrected sensor vs reference method is ~ 0.90 and for PM_{2.5} the R-squared value is ~ 0.95 . In addition, the expanded uncertainty for each correction model, which are estimated at $\sim 10\%$ and $\sim 8\%$ for PM₁₀ and PM_{2.5} respectively for the duration of the study period. The expanded uncertainty threshold recommended by the working group for demonstration of equivalence of a candidate method (CM in Fig. 4) relative to reference method (RM in Fig. 4) is 25%. Similarly, European ambient air quality

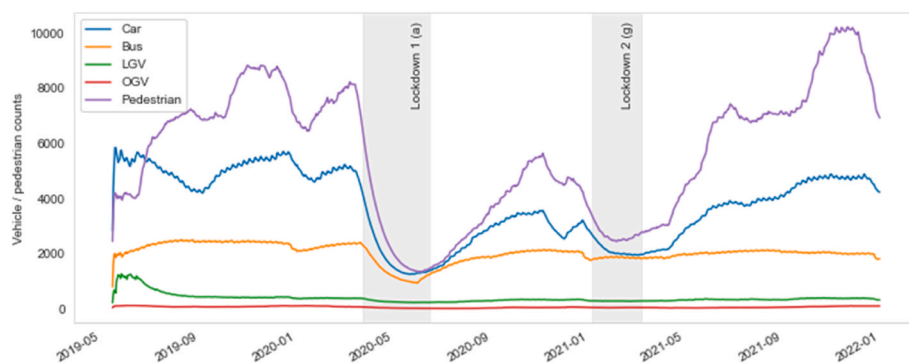


Fig. 4. Smoothed daily mean vehicle and pedestrian flows Oxford, High St. 2019–2022. (Smoothing by exponentially weighted mean at $\alpha = 0.04$).

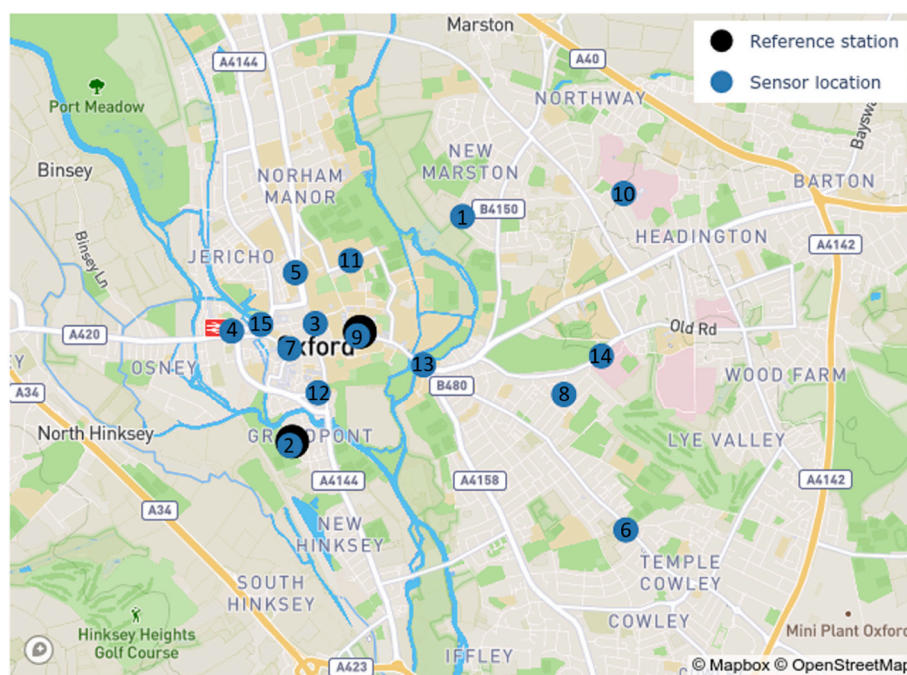


Fig. 5. Map of low-cost air quality sensor and reference measurement locations in Oxford. The numbering corresponds to the sensor locations listed in Table 2.

objectives specify an uncertainty threshold of $\pm 50\%$ for both PM_{10} and $PM_{2.5}$ for indicative monitoring or data to be used to supplement high quality measurements. Within this context, the sensor based PM_{10} and $PM_{2.5}$ datasets produced by this study and corrected with the methods presented, may be regarded as high quality.

3. Results and discussion

3.1. Temporal changes in co-located data

Fig. 8 presents evidence on the adequacy correction methods developed by this study to produce reliable estimates of PM_{10} and $PM_{2.5}$ for the intended comparative application. Fig. 8 presents a timeseries of daily mean PM_{10} and $PM_{2.5}$ for sensor and reference method observations made at the High Street and St Ebbe's monitoring locations. The sensor and reference method baselines and the pre-pandemic baseline for the urban background in Oxford are also shown. The latter is based on the 1-month rolling mean of the mean daily PM concentrations observed by the St Ebbe's reference method in the years 2016–2019. Fig. 8a presents a time series of daily mean PM_{10} at the High St monitoring location for PM_{10} ($PM_{2.5}$ is not measured at this location). From Fig. 8a we observe that the corrected sensor based daily mean PM_{10}

values broadly track those of the reference method, although the sensor trace appears noisy in comparison to that observed at St Ebbe's (Fig. 8b). In addition, there are periods when the corrected High St sensor signal departs from that of the reference method for example in January 2022 when the sensor under-reads relative to the reference and in March and April 2021 when it over-reads relative to the reference. From Fig. 8b and c, we observe that daily mean PM_{10} and $PM_{2.5}$ concentration at St Ebbe's urban background location closely track those of the co-located reference method throughout the study period. The estimated baselines for these observations are likewise shown to be well correlated. The evidence in Fig. 8 and that of the regression analyses in Fig. 7 presents reasonable evidence for the adequacy of the correct sensor data collected by the study for the comparative applications intended.

The estimates of typical daily mean PM_{10} and $PM_{2.5}$ concentrations experienced at urban background locations in Oxford in recent years presented in Fig. 8 (orange line) to contextualise the observations made throughout the 2020/21 lockdown events. Fig. 8a–c provide evidence for PM levels in 2020/21 being comparatively low - Fig. 8a shows the sensor and reference methods observations at the High St roadside location are broadly equivalent to the levels experienced at the urban background in previous years. A similar observation can also be made on Fig. 8b and c, where we see evidence for sensor and reference

Table 2
Sensor deployment by location and environment type.

	Location name	Height	Distance from roadside	Environment type
1	New Marston	4	n/a	Urban background
2	St Ebbe's ^a	2.7	8	Urban background
3	Jesus College	3.3	1.1	Urban intermediate
4	Saïd Business School	9.7	28	Urban intermediate
5	St Giles	5.5	3.5	Urban intermediate
6	Ahlul Bayt Centre	4	10.8	Urban traffic
7	County Hall	5	7.1	Urban traffic
8	Divinity Road	2	7.9	Urban traffic
9	High Street ^a	1.4	3.7	Urban traffic
10	John Radcliffe Hospital	2.75	2.1	Urban traffic
11	South Parks Road	12	7	Urban traffic
12	Speedwell Street	5.9	4.4	Urban traffic
13	The Plain	1.2	9.7	Urban traffic
14	Warneford Hospital	3	4.8	Urban traffic
15	Worcester College	4.7	n/a	Urban traffic

^a Denotes co-located reference location.

measurements in 2020/21 being lower than the average measured at this location between 2016 and 2019.

3.2. Spatial changes over the study period

Fig. 9 presents the frequency distribution of corrected hourly mean particle concentrations for each of the 15 sensor locations in the form of a box plot. The plots present (i) the daily mean IQR as the box element (ii) the median as the horizontal bar inside the IQR, (iii) the mean as the green triangle inside the IQR, (iv) the statistical maxima and minima (defined as 75th percentile \pm 1.5 * the IQR) as the whisker element horizontal endpoints, and (v) outlying sensor observations are shown as black dots (a single marker per outlier observation). In Fig. 9, a consistent distribution in measured PM₁₀ and PM_{2.5} across the sensor network is observed; the sensor datasets are skewed in a manner frequently seen in particles datasets, with an asymmetrical right-skewed probability density function (approaching a lognormal distribution). The mean PM₁₀ concentration over the duration of the study and across the network was 11 $\mu\text{g}/\text{m}^3$ (SD \pm 5.9 $\mu\text{g}/\text{m}^3$), and mean PM_{2.5} concentrations was 8 $\mu\text{g}/\text{m}^3$ (SD \pm 5.9 $\mu\text{g}/\text{m}^3$). The full dynamic range in hourly PM₁₀ was 4–75 $\mu\text{g}/\text{m}^3$, and 1–50 $\mu\text{g}/\text{m}^3$ for PM_{2.5}, although for as shown by the whisker elements of the plots, after excluding data points that can be reasonably assumed to be outliers the likely dynamic range

Table 3
Summary of Random Forest hyperparameter setting used in model training.

Hyperparameter	Model Type	
	PM ₁₀	PM _{2.5}
No. of trees	100	100
Criterion	0	0
Max. tree depth	0	0
Min. samples per leaf node	1	1
Max. no. of leaf nodes	6,000	4,000
Min. sample per node	2	2
Min. leaf node weight fraction	0	0
Min. impurity decrement	0	0
Min impurity split	0	0
Max. no. features (see Bush et al. [31] for the derivation of feature used)	15	15
No. jobs	–1	–1
Bootstrap sampling	1	1
Training sample population	n = 46,032 (High St and St Ebbe's)	n = 30,902 (St Ebbe's)

in the 1-h mean is approximately 4–35 $\mu\text{g}/\text{m}^3$ (PM₁₀) and 1–30 $\mu\text{g}/\text{m}^3$ (PM_{2.5}). The propensity for right skewed data in Fig. 9a and b (including outliers) whilst typical of air quality datasets may also be indicative of sensor performance issues (e.g. interferences from temperature, relative humidity, low sample volume) and a limitations in the training of the RF correction model which has undercompensated for the interference(s). Outliers may also arise from individual effects at sensors, for example a parked, idling vehicle or a person smoking a cigarette. The mean interquartile range (IQR) for both PM₁₀ and PM_{2.5} was \sim 6 $\mu\text{g}/\text{m}^3$ SD (\pm 1.7 $\mu\text{g}/\text{m}^3$), indicating that the bulk of the observations are of a similar sample population.

Fig. 9 also illustrates a small local impact from traffic related emission sources upon particle concentrations near traffic-oriented sensors. At these locations we observe higher average and peak concentrations and the IQR is broader from traffic-oriented sensors than that displayed by more intermediate and background orientated sensor locations. The greater dynamic range in concentrations is indicative of exposure to more variable emission sources, such as road transport emissions, and correlates well with the sensor proximity to traffic emissions (Table 2).

Notwithstanding the variations above, Fig. 9 shows evidence for differing PM₁₀ and PM_{2.5} behaviours across the sensor network; demonstrating the value of a multi-sensor network to assess spatial differences in PM patterns and trends over the study period. PM_{2.5} values are broadly constant and of the same dynamic range throughout the network - PM_{2.5} levels from the urban background reference station are representative of all a few of the locations measured in this study. These locations (Ahlul Bayt, High Street, South Parks Road, and Worcester College) are all located on particularly busy roads with (in the case of Ahlul Bayt and High Street) high levels of bus and HGV traffic. With PM₁₀, however, there is greater dynamic range in observation, with differences of a factor of approximately 1.7 visible across the network. The same four locations show higher levels of PM₁₀ as does the John Radcliffe hospital, a site with construction being undertaken during the period measured and a combined heat and power (CHP) generation plant located on-site (the stack from the CHP plant is approximately 250 m from the location of the sensor).

3.3. Proximity of measured concentrations in relation to annual limit and guideline values

Fig. 10 presents the range and distribution of daily mean PM₁₀ and PM_{2.5} concentrations measured at each sensor location for a 12-month period from the study (July 2020 to June 2021). Restricting the study dataset to 12-months facilitates comparison with air quality objectives, limits and guideline values which are based on calendar year datasets [8, 37]. Fig. 10a shows that the majority of daily mean PM₁₀ observations are well below both the 45 $\mu\text{g}/\text{m}^3$ WHO guideline level and 50 $\mu\text{g}/\text{m}^3$ UK Air Quality Objective (the latter not to be exceeded >35 times in a calendar year). Furthermore, because all (upper) whisker elements terminate below the 50 $\mu\text{g}/\text{m}^3$ (at least 15 $\mu\text{g}/\text{m}^3$ below) it is only sensor observations that can be reasonably classified as outliers that approach or more rarely exceed the thresholds above; good evidence that the daily mean PM₁₀ health protection thresholds are rarely exceeded in Oxford.

Fig. 10b presents similar information for daily mean PM_{2.5} for which the WHO have set a guideline value of 15 $\mu\text{g}/\text{m}^3$ [8]; there are no UK or European legislative thresholds set for this pollutant and averaging period. Fig. 10b shows that although the majority of daily mean PM_{2.5} observations are \leq 15 $\mu\text{g}/\text{m}^3$, the upper bounds of IQR (i.e. the 75th percentile concentration value) are \leq 15 $\mu\text{g}/\text{m}^3$, higher percentile concentrations do exceed the WHO guideline value. These data provide good evidence to indicate that the 15 $\mu\text{g}/\text{m}^3$ daily mean WHO guide value for PM_{2.5} was regularly exceeded in 2020/21 despite the lockdown conditions, reduced traffic volumes (see Fig. 4) and associated emissions.

Fig. 11 presents annual mean PM₁₀ and PM_{2.5} concentrations measured over the same 12-month period. Relevant UK, European and

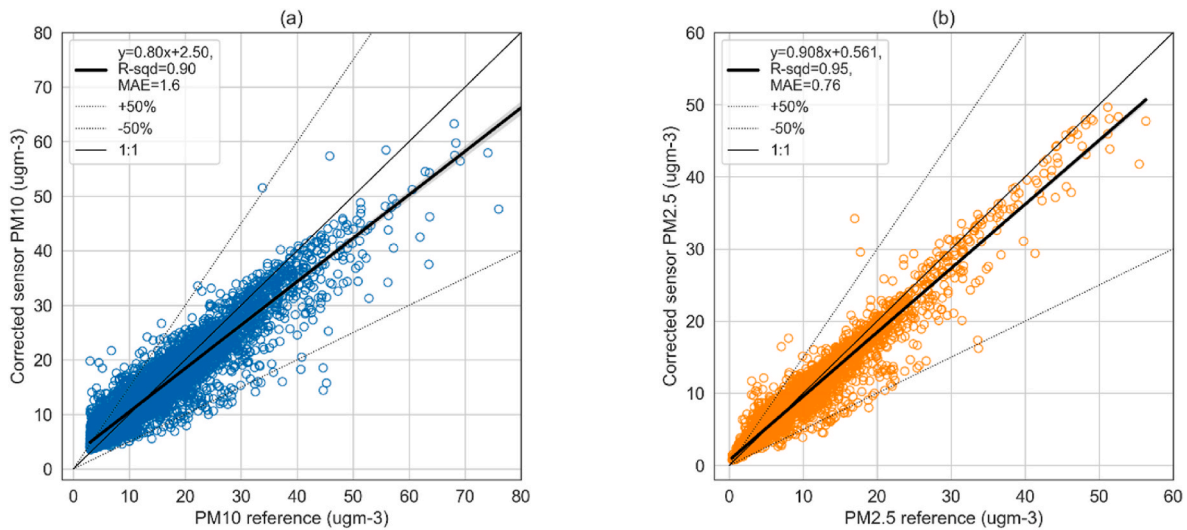


Fig. 6. Regression analysis of corrected (a) PM_{10} , (b) $PM_{2.5}$ sensor data from co-located sensor and reference method observations for the duration of the study.

Table 4

Comparison in performance of sensors before and after RF correction method [31].

	Mean absolute error (MAE)		Coefficient of determination (R^2)		Improvement in MAE arising from RF correction model
	Baseline	RF correction model	Baseline	RF correction model	
PM_{10} ($\mu\text{g}/\text{m}^3$)	34.6	1.6	0.01	0.90	95%
$PM_{2.5}$ ($\mu\text{g}/\text{m}^3$)	8.9	0.76	0.28	0.95	91%

WHO thresholds are again shown as dashed horizontal lines for both PM_{10} and $PM_{2.5}$. Fig. 11a and b Measured annual mean concentrations are well below regulatory UK and European threshold values for both PM_{10} ($40 \mu\text{g}/\text{m}^3$) and $PM_{2.5}$ ($25 \mu\text{g}/\text{m}^3$). Similarly, Fig. 11a shows that annual mean PM_{10} concentrations at all locations were below the WHO

2005 guide value ($20 \mu\text{g}/\text{m}^3$), and all but two locations (High Street and South Parks Road) were below the more stringent 2021 revised guide value ($15 \mu\text{g}/\text{m}^3$). Fig. 11b shows that there was widespread exceedance of the 2021 revised WHO guideline value for annual mean $PM_{2.5}$ ($5 \mu\text{g}/\text{m}^3$), whereas only three sensor locations, Divinity Road, High Street, South Parks Road exceeded the 2005 guide value ($10 \mu\text{g}/\text{m}^3$ as an annual mean), which is also the UK $PM_{2.5}$ legally binding objective. Again, these data provide strong evidence that despite lower traffic volumes during 2020/21 (see Fig. 4) the 2021 WHO annual mean guideline value for PM_{10} was approached or exceeded close to busy roads in Oxford and there was widespread exceedance of the same guideline value for $PM_{2.5}$, a level that is the new legally binding Air Quality Objective in the UK. These findings indicate that additional non-traffic related measures would be required in Oxford to reduce the PM_{10} and $PM_{2.5}$ levels to within health-based guidelines and to achieve compliance with forthcoming legally binding objectives.

3.4. Identifying changes in particle concentrations linked to COVID-19 restriction events

Figs. 12 and 13 present a heat-map based analysis of the variation in

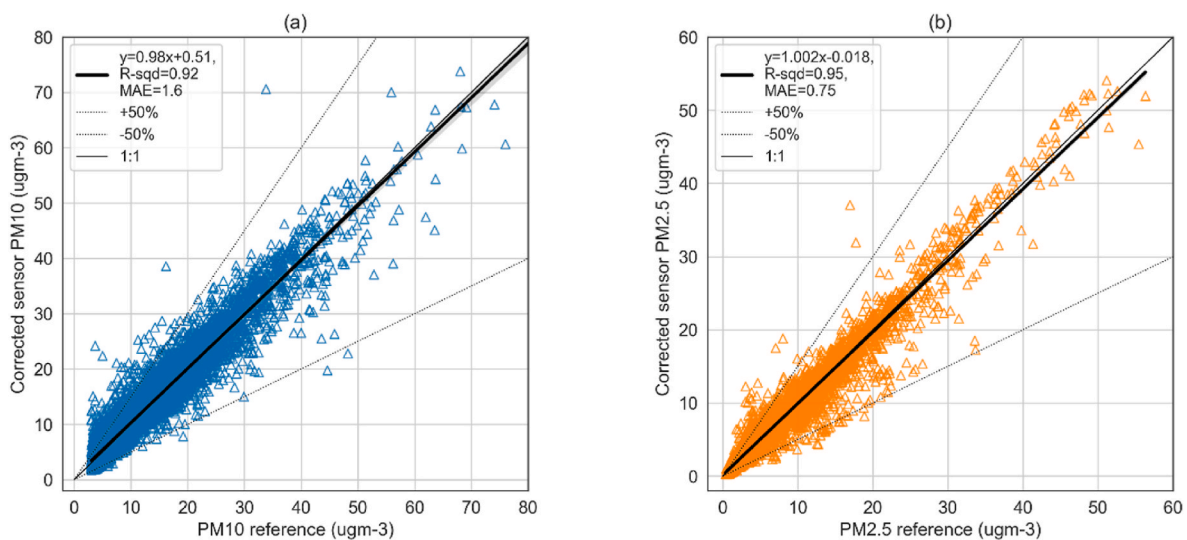


Fig. 7. Regression analysis of final corrected sensor data from co-located sensor and reference method observations for the duration of the study with gradient and intercept correction applied. (a) PM_{10} , (b) $PM_{2.5}$.

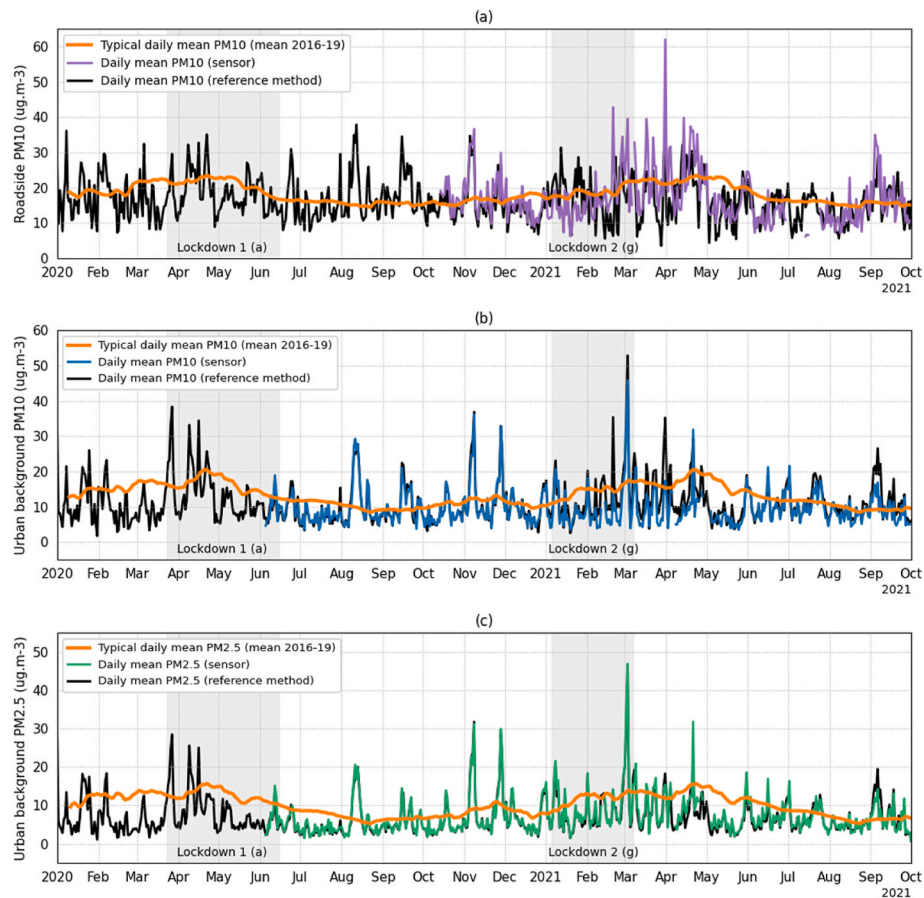


Fig. 8. Time series of co-located sensor and reference method PM₁₀ and PM_{2.5} measurements showing the deviations from the baseline over the study period and comparing of the corrected sensor data with corresponding reference measurement. (a) PM₁₀ at the High St monitoring station, (b) PM₁₀ at the St Ebbe's monitoring station, (c) PM_{2.5} at the St Ebbe's monitoring station.

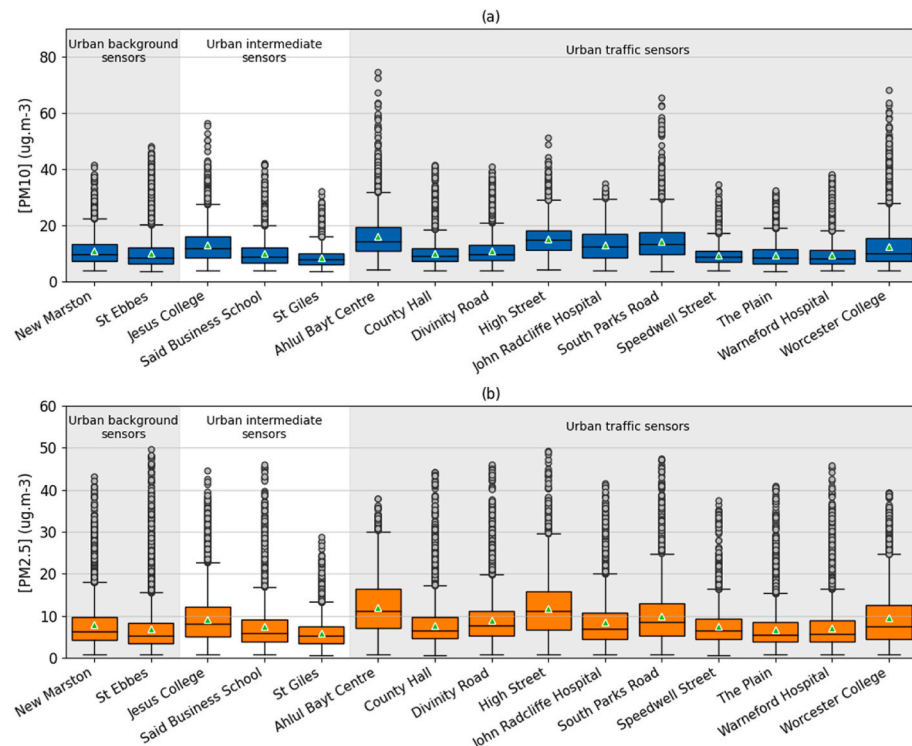


Fig. 9. Frequency distribution of corrected hourly mean particle concentrations by sensor. (a) PM₁₀, (b) PM_{2.5}.

mean PM concentrations measured during the COVID-19 public health restriction events of 2020-21 (restriction events have been previously defined in Table 2). Measured PM levels are compared with the 2016-19 pre-pandemic baseline. Differentials in mass concentration for the daily mean and 95th percentile value of hourly observations were calculated for each sensor and restriction event. Statistical significance in each differential is indicated by shading; shaded cells are not significantly different at 95% confidence, whereas unshaded cells are.

Fig. 12 illustrates several patterns in measured PM concentrations during the COVID-19 restriction events of 2020-21 relative to the baseline. Clearly, there is a marked variability in the differences shown both across the sensor network (the vertical axis) and over lockdown events (the horizontal axis), this is more evident in the daily means (using the scales shown). Peak concentrations, represented by the mean daily 95th percentile (Fig. 13), are in general consistently lower than baseline urban background levels throughout all lockdown events. On average, peak concentrations of PM₁₀ were $\sim 10 \mu\text{g}/\text{m}^3$ lower than baseline values ($\text{SD} \pm 6.0 \mu\text{g}/\text{m}^3$), peak concentrations found on corresponding days in previous years. Similarly, peak PM_{2.5} levels were $\sim 9 \mu\text{g}/\text{m}^3$ ($\text{SD} \pm 3.0 \mu\text{g}/\text{m}^3$) lower than concentrations observed on corresponding days in recent years. There was no overall trend for any sensor showing increases in peak concentrations relative to the baseline of statistical significance.

This variability between peak (95th percentile) and mean concentrations is interesting. Perhaps by removing much traffic from the roads, the peak values, which may be caused only by a few “gross emitters” (vehicles which make up a small minority of the fleet but can account for substantial emissions [57]), have fallen, but given the low contribution of traffic to the overall PM in Oxford [58], the mean levels are much less affected. Given that recent studies on the health impacts of acute compared to chronic exposure indicate that chronic exposure is more important for public health [59], this would suggest that measures targeting traffic reduction in isolation may not be the most effective in this setting for improving population health.

Some of the variability in daily mean differentials may be

demarcated by local emission sources and sensor location classifications. On the vertical axis sensor locations closer to roads and influenced by hyper-local road transport emissions present concentrations consistently above the baseline (remember that the baseline is an urban background baseline), whereas urban background locations display concentrations consistently below the baseline.

The comparable differentials displayed by High Street and Divinity Road are notable given the local setting of each. The High Street location is a roadside location in central Oxford with $\sim 16,400$ vehicle flows per day. Given these conditions, the positive differential at this location relative to baseline concentrations is expected. Conversely, Divinity Road is a narrow, minor road in a residential area of East Oxford. It is interesting to note, therefore, that the levels observed at Divinity Road during the periods of restrictions were only marginally less than those found at the High Street; although neither can be shown to be significantly different from the baseline in some periods (see shading in Fig. 8). Further local knowledge of the locations reveals that Divinity Road has a steep incline and is known locally as a traffic and pollution hotspot – the road is frequently used as a cut through/rat run by local traffic at all times of the day and evidentially similar levels to those of a traffic orientated location. Given the residential area (indeed the sensor is mounted on a residential property) this may have importance for residents' exposure to PM.

On the horizontal axes of Fig. 8 it is possible to track the variation in PM levels over the course of successive restriction events relative to typical concentrations from previous years. Although it is observed that the sensor network was not fully commissioned in time to capture the transition into ‘lockdown’ at all locations, there is evidence from three locations over this period. Notably, there is some statistically significant evidence of levels of daily mean PM₁₀ and PM_{2.5} being elevated relative to the baseline during the 1st national lockdown, (event ‘b’ from 23 March 2020).

After the 1st national lockdown, events ‘c’ to ‘d’ correspond to the gradual easing of restrictions (schools returning, retail opening etc.) and subsequently the introduction of tiered locally tuned restriction

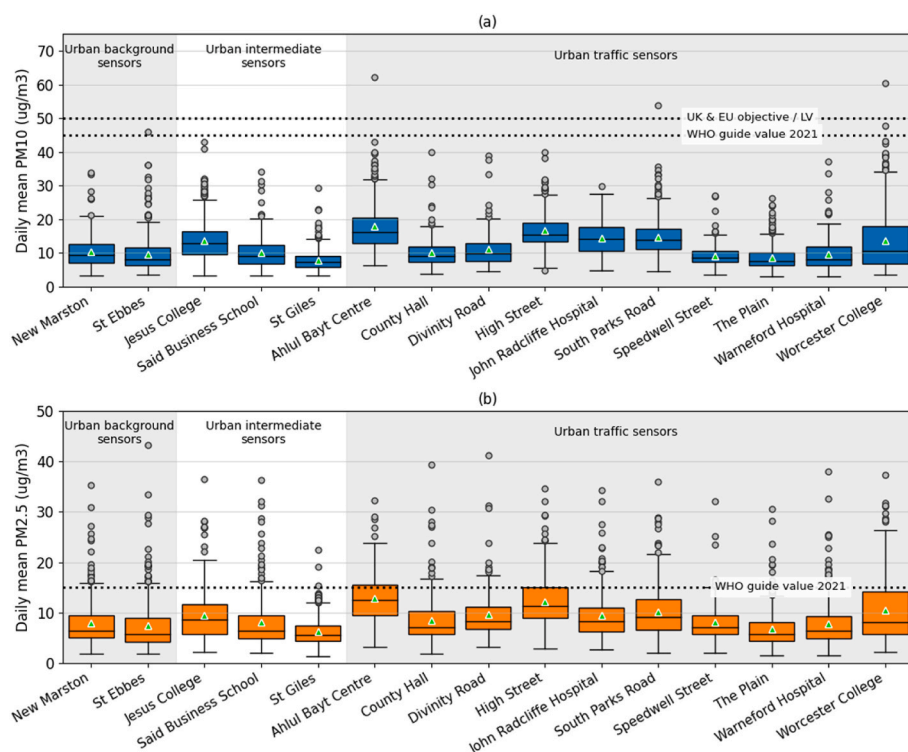


Fig. 10. Frequency distribution of daily mean PM₁₀ and PM_{2.5} concentrations measured over at sensor location during a 12-month period. (a) daily mean PM₁₀, (b) daily mean PM_{2.5}

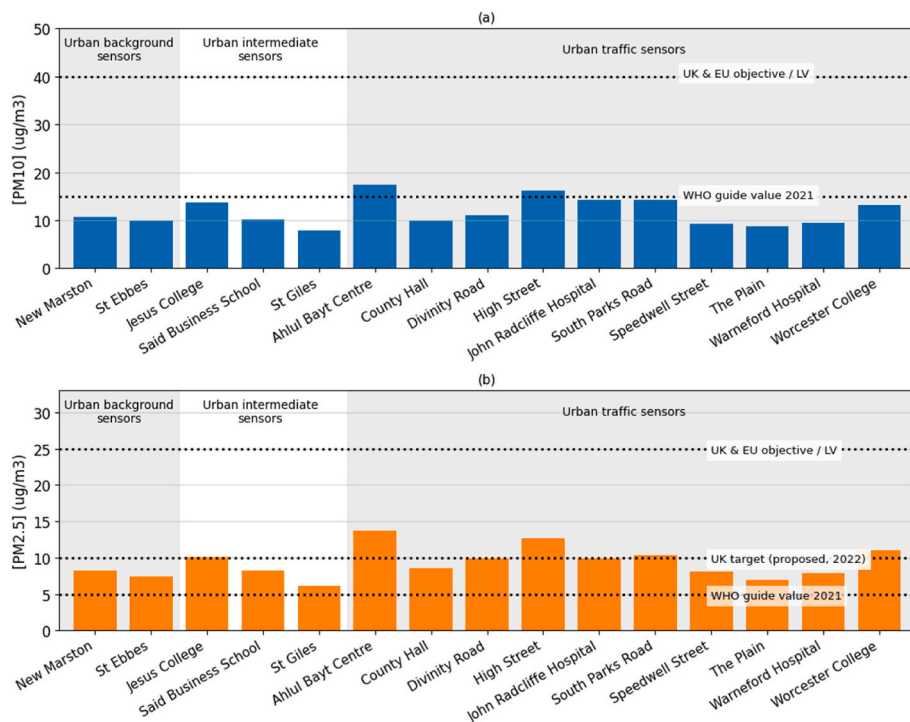


Fig. 11. Measured annual mean PM₁₀ and PM_{2.5} concentrations over the 12 months July 2020 to June 2021 with corresponding annual mean objectives and guide values indicated. (a) annual mean PM₁₀, (b) annual mean PM_{2.5}.

measures (from 10 May 2020 and 24 September 2020 respectively). During this period there is statistically significant evidence of daily mean and peak levels being lower than the baseline. Lockdown events 'e' and 'f' (National lockdown-2 and Tier 2 to 4 local restrictions for Oxford on 5 November 2020 and 2 December 2020) coincide with daily mean and, to a lesser degree, peak concentrations levels above the baseline throughout the sensor network although these observations are not generally statistically significant (at $P = 0.05$). December 2020 was followed, by periods when mean and peak concentrations throughout Oxford were lower than the baseline and there is marked consistency and statistical significance in this trend over this period, particularly for

peak PM concentrations. Events 'g' to 'i' correspond to the introduction of National lockdown-3 and Steps 1 and 2 out of lockdown, from 5 Jan 2021 to 17 May 2021. Note that, these events and the observed levels coincided with periods of the year that normally exhibit seasonal maxima, thus indicating that PM levels in first quarter of 2021 (i.e. pre-pandemic restrictions) were typically low compared with the baseline. During lockdown periods 'j' and 'k' (Step-3 out of lockdown 17 May 2021 and 'Freedom Day' 21 June 2021 respectively) the lower concentrations observed in quarter 1 of 2021 had returned close to typical baseline levels.

This study is not, however, able to make a direct link between traffic

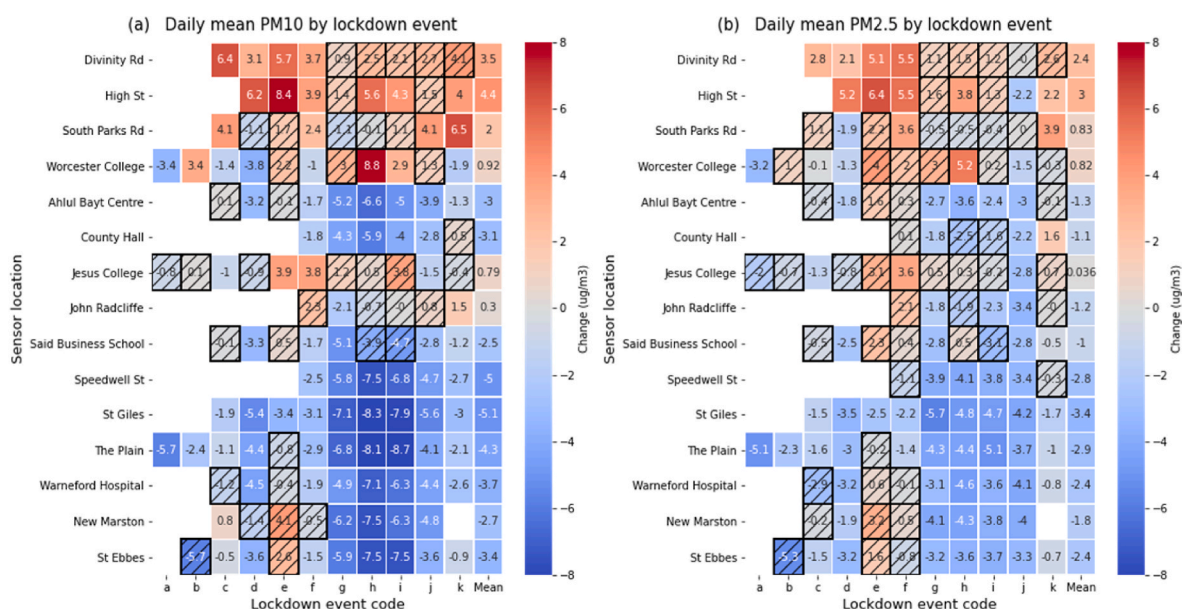


Fig. 12. Heat map representation of the differential in daily mean PM during COVID-19 pandemic restriction events 2020/21 relative to the baseline. (a) Daily mean PM₁₀, (b) Daily mean PM_{2.5}. Differences shown in $\mu\text{g}/\text{m}^3$. All changes are statistically significant unless denoted by shading.

levels and PM pollution at a specific location, because PM and traffic counting has not been directly co-located, however such a study would be a clear next step for this work. Similarly, the data is not able to apportion the source of the PM explicitly, further work and alternative techniques could be applied in order to further understand the sources of the PM in Oxford and whether there is significant spatial and/or temporal variation. Finally, PM is hardly the only pollutant to affect human health, and so future work should consider additional pollutants such as oxides of nitrogen, ozone, and other harmful pollutants.

4. Summary and conclusions

In this study, a network of low-cost particle sensors has been deployed at 15 locations in the city of Oxford. A random forest machine learning algorithm has been used to provide robust high-quality data for PM₁₀ and PM_{2.5}, demonstrating that the data used are compliant with European ambient air quality directive [38] objectives for uncertainty. The impact of public health induced restrictions associated with the COVID-19 pandemic on PM₁₀ and PM_{2.5} levels has been explored across network data over the period January 2020 to September 2021.

The study evidence draws several conclusions:

1. There is evidence for a reduction in PM levels in 2020/21 in Oxford compared to previous years. Specifically, we identified modest reductions in daily average PM₁₀ and PM_{2.5} concentrations ($\sim 1 \mu\text{g}/\text{m}^3$) and more substantive reductions ($9\text{--}10 \mu\text{g}/\text{m}^3$) in peak concentrations from the pre-pandemic baseline. These findings suggest that traffic reduction associated with public health restrictions may have had an impact on peak morning and evening concentrations; and therefore benefits for reducing short-term pollutant exposures among those living in the city.
2. There was marked spatial and temporal variability in PM₁₀ and PM_{2.5} observations throughout the COVID-19 emergency restrictions of 2020–21. The highest PM₁₀ and PM_{2.5} levels were still measured at roadside locations, despite major traffic reductions during public health restrictions
3. PM₁₀ concentrations rarely exceed World Health Organisation Global Air Quality Guidelines for annual mean or 24-h concentrations in Oxford City, even at roadside locations. However, WHO

guideline annual mean and 24-h concentrations for PM_{2.5} were widely exceeded throughout the sensor network during public health restrictions, including at residential locations. All but three locations were compliant with the long-term UK target for PM_{2.5} (annual mean $10 \mu\text{g}/\text{m}^3$). Given the disparity in peak compared to mean PM₁₀ and PM_{2.5} reductions, and the source apportionment of PM₁₀ and PM_{2.5} in Oxford (including major contribution of non-transport sources), additional measures to deliver emissions reductions will be required to reduce annual average concentrations towards WHO health-based guidelines.

4. Some sensor network locations exhibited atypical behaviours (concentrations) when taken in the context of their general environment; for example a sensor location based in residential areas exhibiting levels of PM₁₀ and PM_{2.5} consistent with heavily trafficked city-centre roadside locations. This demonstrates the value of a sensor network approach for generating high spatial resolution air quality data to identify pollution hotspots, which can be the focus for future intervention measures.

These observations agree with the findings of other studies [15] which showed that despite achieving 70% reduction in city centre traffic volume, Oxford's COVID-19 emergency restrictions had negligible impact upon long-term PM levels (after accounting for seasonal and meteorological influences) with indication of an increase in PM₁₀ during the second national lockdown. This is consistent with and indicative of the source apportionment characteristics for PM in Oxford where agriculture and domestic heating play a more prominent role in the contribution to ambient PM.

The natural experiment opportunity presented by multiple COVID-19 pandemic emergency measures has shown that measures restricting emissions from road traffic will not significantly reduce PM₁₀ or PM_{2.5} concentrations in Oxford (or likely elsewhere in the UK). As a result, other interventions will be needed to reduce long term PM concentrations, of benefit for human health. Specifically, sources to be targeted for further interventions to reduce PM levels include fossil fuel based commercial and residential heating and agriculture.

We have demonstrated the utility of high spatial resolution low-cost sensor networks for the acquisition of, high quality evidence on PM₁₀ and PM_{2.5} levels in an urban setting. The sampling capabilities of the

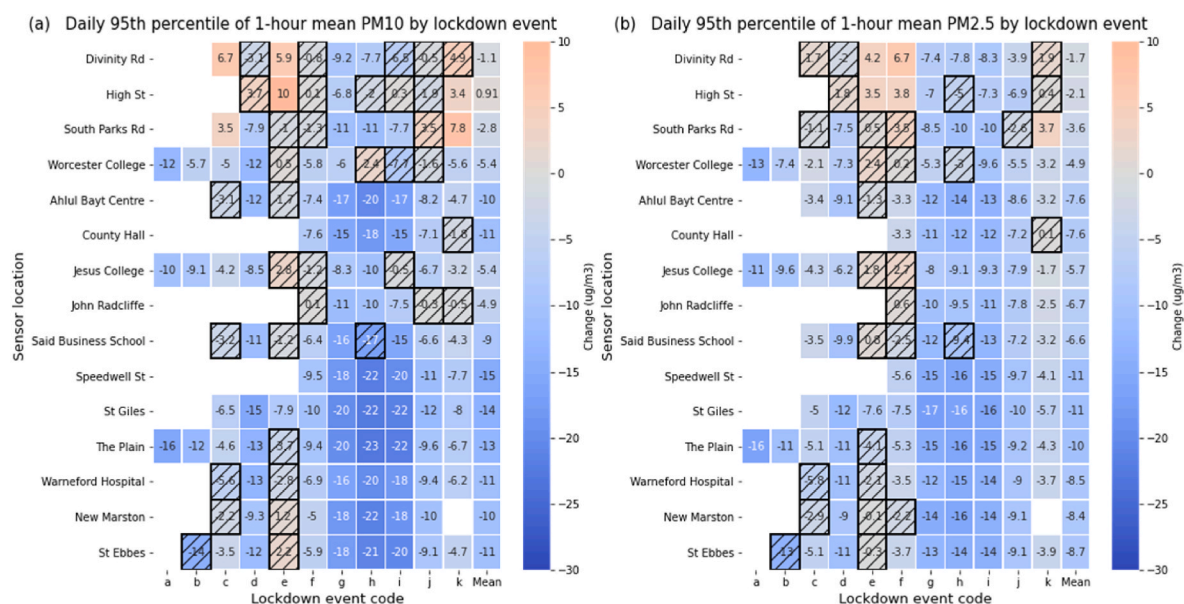


Fig. 13. Heat map representation of the differential in daily 95th percentile of 1-h mean PM during COVID-19 pandemic restriction events 2020/21 relative to the baseline. (a) Daily 95th percentile of 1-h mean PM₁₀, (b) Daily 95th percentile of 1-h mean PM_{2.5}. Differences shown in $\mu\text{g}/\text{m}^3$. All changes are statistically significant unless denoted by shading.

sensing techniques used have facilitated the characterisation of both hourly peak, daily and long-term mean and mode PM levels and these have been contextualised against historical measurements in Oxford using reference instrumentation from recent years. The convenience of the sensing technologies used has allowed sampling to be carried out over a diverse network of monitoring locations and typical local conditions in Oxford. The sensor network and supporting data processing techniques have enabled the impact of altered patterns in economic activity and travel behaviours arising from the COVID-19 emergency restriction measures within the Oxford to be understood with a high degree of certainty.

Funding

This research was funded by The Natural Environment Research Council, grant number NE/V010360/1. Its forerunning pilot project was funded by The National Institute for Health Research (NIHR), grant number NIHR130095. The views expressed are those of the author(s) and not necessarily those of the NIHR or the Department of Health and Social Care. This publication arises in part from research funded by Research England's Strategic Priorities Fund (SPF) QR allocation.

CRediT authorship contribution statement

Tony Bush: Writing – original draft, Formal analysis, Data curation, Conceptualization. **Suzanne Bartington:** Writing – review & editing, Supervision, Funding acquisition, Conceptualization. **Francis D. Pope:** Writing – review & editing, Supervision, Funding acquisition. **Ajit Singh:** Writing – review & editing, Formal analysis. **G. Neil Thomas:** Writing – review & editing, Funding acquisition. **Brian Stacey:** Writing – review & editing, Investigation, Data curation. **George Economides:** Writing – review & editing, Resources, Data curation. **Ruth Anderson:** Writing – review & editing, Resources, Data curation. **Stuart Cole:** Writing – review & editing, Resources, Data curation. **Pedro Abreu:** Writing – review & editing, Data curation. **Felix C.P. Leach:** Writing – review & editing, Writing – original draft, Supervision, Funding acquisition, Data curation, Conceptualization.

Declaration of competing interest

The authors declare the following financial interests/personal relationships which may be considered as potential competing interests:

Felix Leach reports financial support was provided by Natural Environment Research Council, The National Institute for Health Research, and Research England's Strategic Priorities Fund (SPF) QR allocation.

Data availability

Data is available through ORA and CEDA.

Raw data for Figures for The impact of COVID-19 public health restrictions on particulate matter pollution measured by a validated low-cost sensor network in Oxford, UK https://deposit.ora.ox.ac.uk/concern/datasets/uuid_3ea5302b-c151-4c35-a4b7-0269c36fbd9c?locale=en

Acknowledgments

The authors would like to extend thanks and gratitude to the Chair of the study Steering Committee, the late Prof Martin Williams, for his guidance and encouragement over the years. The authors would also like to thank the study steering committee for their technical contributions and administrative support and Ricardo Energy & Environment in facilitating data acquisition. Oxford City Council and Oxfordshire County Council are thanked for advice and support in deployment of

several sensors. The following individuals and organisations hosting or facilitating the hosting of sensors: the Quaker Meeting House, St Giles; St Ebbe's Primary School; the Ahlul Bayt Centre; Divinity Road residents; the John Radcliffe Hospital; the Warneford Hospital; Jesus College; Worcester College; Magdalen College; the Said Business School; Oxfordshire County Council offices (Speedwell St and County Hall); the School of Geography and the Environment, Oxford.

Nomenclature

AIRPLS	Adaptive Iteratively Reweighted Penalized Least Squares
AURN	Automated Urban and Rural Network
AQMA	Air Quality Management Area
CHP	Combined Heat and Power
CM	Candidate Method
COVID-19	Coronavirus disease
FDMS	Filter Dynamics Measurement System
IQR	Inter-Quartile Range
LEZ	Low Emission Zone
ML	Machine Learning
OPC	Optical Particle Counter
PM	Particulate M < atter
PM _{2.5}	Fraction of PM where particles are less than 2.5 µm in diameter
PM ₁₀	Fraction of PM where particles are less than 10 µm in diameter
RF	Random Forest
RM	Reference Method
SARS-CoV-2	Severe Acute Respiratory Syndrome Coronavirus 2
SD	Standard Deviation
UK	United Kingdom
WHO	World Health Organisation
ZEZ	Zero Emission Zone

References

- [1] Defra, Clean Air Strategy. <https://www.gov.uk/government/publications/clean-air-strategy-2019>, 2019.
- [2] C.M. Wong, et al., Cancer mortality risks from long-term exposure to ambient fine particle, *Cancer Epidemiol. Biomarkers Prev.* 25 (5) (2016) 839–845, <https://doi.org/10.1158/1055-9965.Epi-15-0626>.
- [3] J. Chen, G. Hoek, Long-term exposure to PM and all-cause and cause-specific mortality: a systematic review and meta-analysis, *Environ. Int.* 143 (2020), 105974, <https://doi.org/10.1016/j.envint.2020.105974>.
- [4] P. Orellano, et al., Short-term exposure to particulate matter (PM₁₀ and PM_{2.5}), nitrogen dioxide (NO₂), and ozone (O₃) and all-cause and cause-specific mortality: systematic review and meta-analysis, *Environ. Int.* 142 (2020), 105876, <https://doi.org/10.1016/j.envint.2020.105876>.
- [5] M.A. Shehab, F.D. Pope, Effects of short-term exposure to particulate matter air pollution on cognitive performance, *Sci. Rep.* 9 (1) (2019) 8237, <https://doi.org/10.1038/s41598-019-44561-0>.
- [6] X. Gao, et al., Short-term air pollution, cognitive performance and nonsteroidal anti-inflammatory drug use in the Veterans Affairs Normative Aging Study, *Nature Aging* 1 (5) (2021) 430–437, <https://doi.org/10.1038/s43587-021-00060-4>.
- [7] Royal College of Physicians. Every Breath We Take: the Lifelong Impact of Air Pollution, 2016. <https://www.rcplondon.ac.uk/projects/outputs/every-breath-we-take-lifelong-impact-air-pollution>.
- [8] World Health Organization, WHO Global Air Quality Guidelines: Particulate Matter (PM_{2.5} and PM₁₀), Ozone, Nitrogen Dioxide, Sulfur Dioxide and Carbon Monoxide, World Health Organization, Geneva, 2021. <https://apps.who.int/iris/handle/10665/345329>.
- [9] WHO. Listings of WHO's response to COVID-19, Available from: <https://www.who.int/news/item/29-06-2020-covid-timeline>, 2021. (Accessed 29 September 2022).
- [10] F. Fu, K.L. Purvis-Roberts, B. Williams, Impact of the COVID-19 pandemic lockdown on air pollution in 20 major cities around the world, *Atmosphere* 11 (11) (2020) 1189.
- [11] R.S. Sokhi, et al., A global observational analysis to understand changes in air quality during exceptionally low anthropogenic emission conditions, *Environ. Int.* 157 (2021), 106818, <https://doi.org/10.1016/j.envint.2021.106818>.
- [12] Z.S. Venter, et al., COVID-19 lockdowns cause global air pollution declines, *Proc. Natl. Acad. Sci. USA* 117 (32) (2020) 18984–18990, <https://doi.org/10.1073/pnas.2006853117>.
- [13] C. Jephcote, et al., Changes in air quality during COVID-19 'lockdown' in the United Kingdom, *Environ. Pollut.* 272 (2021), 116011, <https://doi.org/10.1016/j.envpol.2020.116011>.

- [14] Z. Shi, et al., Abrupt but smaller than expected changes in surface air quality attributable to COVID-19 lockdowns, *Sci. Adv.* 7 (3) (2021) eabd6696, <https://doi.org/10.1126/sciadv.abd6696>.
- [15] A. Singh, et al., Impacts of emergency health protection measures upon air quality, traffic and public health: evidence from Oxford, UK, *Environ. Pollut.* 293 (2022), 118584, <https://doi.org/10.1016/j.envpol.2021.118584>.
- [16] S. Zangari, et al., Air Quality Changes in New York City during the COVID-19 Pandemic, 742, *Science of The Total Environment*, 2020, 140496, <https://doi.org/10.1016/j.scitotenv.2020.140496>.
- [17] N. Castell, et al., Can commercial low-cost sensor platforms contribute to air quality monitoring and exposure estimates? *Environ. Int.* 99 (2017) 293–302, <https://doi.org/10.1016/j.envint.2016.12.007>.
- [18] G. Fanti, et al., Evolution and applications of recent sensing technology for occupational risk assessment: a rapid review of the literature, *Sensors* 22 (13) (2022) 4841.
- [19] F. Borghi, et al., Miniaturized monitors for assessment of exposure to air pollutants: a review, *Int. J. Environ. Res. Publ. Health* 14 (8) (2017) 909.
- [20] F.C.P. Leach, M.S. Peckham, M.J. Hammond, Identifying NOx hotspots in transient urban driving of two diesel buses and a diesel car, *Atmosphere* 11 (4) (2020) 355.
- [21] P. Schneider, et al., Mapping urban air quality in near real-time using observations from low-cost sensors and model information, *Environ. Int.* 106 (2017) 234–247, <https://doi.org/10.1016/j.envint.2017.05.005>.
- [22] G. Fanti, et al., Features and practicability of the next-generation sensors and monitors for exposure assessment to airborne pollutants: a systematic review, *Sensors* 21 (13) (2021) 4513.
- [23] Y. Kang, et al., Performance Evaluation of Low-Cost Air Quality Sensors: A Review, 818, *Science of The Total Environment*, 2022, 151769, <https://doi.org/10.1016/j.scitotenv.2021.151769>.
- [24] J. Howard, et al., Advanced sensor technologies and the future of work, *Am. J. Ind. Med.* 65 (1) (2022) 3–11, <https://doi.org/10.1002/ajim.23300>.
- [25] L. Morawska, et al., Applications of low-cost sensing technologies for air quality monitoring and exposure assessment: how far have they gone? *Environ. Int.* 116 (2018) 286–299, <https://doi.org/10.1016/j.envint.2018.04.018>.
- [26] D. Bousiotis, et al., Assessing the sources of particles at an urban background site using both regulatory instruments and low-cost sensors – a comparative study, *Atmos. Meas. Tech.* 14 (6) (2021) 4139–4155, <https://doi.org/10.5194/amt-14-4139-2021>.
- [27] D.H. Hagan, J.H. Kroll, Assessing the accuracy of low-cost optical particle sensors using a physics-based approach, *Atmos. Meas. Tech.* 13 (11) (2020) 6343–6355, <https://doi.org/10.5194/amt-13-6343-2020>.
- [28] Defra, Environment Act, 2021, 2021, <https://www.legislation.gov.uk/ukpga/2021/30/contents>.
- [29] S. Wang, et al., Mobile monitoring of urban air quality at high spatial resolution by low-cost sensors: impacts of COVID-19 pandemic lockdown, *Atmos. Chem. Phys.* 21 (9) (2021) 7199–7215, <https://doi.org/10.5194/acp-21-7199-2021>.
- [30] E. Chadwick, et al., Technical note: understanding the effect of COVID-19 on particle pollution using a low-cost sensor network, *J. Aerosol Sci.* 155 (2021), 105766, <https://doi.org/10.1016/j.jaerosci.2021.105766>.
- [31] T. Bush, et al., Machine learning techniques to improve the field performance of low-cost air quality sensors, *Atmos. Meas. Tech.* 15 (10) (2022) 3261–3278, <https://doi.org/10.5194/amt-15-3261-2022>.
- [32] ONS, Population Estimates, 2019. Available from: <https://www.ons.gov.uk/peop-lepopulationandcommunity/populationandmigration/populationestimates>. (Accessed 29 September 2022).
- [33] Oxford City Council, Oxford's Population, 2022. Available from: <https://www.oxford.gov.uk/info/20131/population/459/oxfords-population>. (Accessed 29 September 2022).
- [34] Oxford City Council, Air Quality Action Plan 2021–2025, 2021. <https://www.oxford.gov.uk/downloads/file/7428/air-quality-action-plan-2021-2025>. (Accessed 29 September 2022).
- [35] Oxford City Council, Background to the Oxford Zero Emission Zone, (ZEZ), 2022. <https://www.oxford.gov.uk/info/20299/air-quality-projects/1305/background-to-the-oxford-zero-emission-zone-zez>. (Accessed 29 September 2022).
- [36] Defra, Air Quality PM2.5 Targets: Detailed Evidence Report, 2022.
- [37] Defra, The Air Quality Strategy for England, Scotland, Wales and Northern Ireland, 2007.
- [38] European Parliament, Directive 2008/50/EC of the European Parliament and of the Council of 21 May 2008 on Ambient Air Quality and Cleaner Air for Europe, 2008.
- [39] P. Virtanen, et al., SciPy 1.0: fundamental algorithms for scientific computing in Python, *Nat. Methods* 17 (3) (2020) 261–272, <https://doi.org/10.1038/s41592-019-0686-2>.
- [40] Age UK, Lockdown Extension: Coronavirus Roadmap Delayed, 2021. Available from: <https://www.ageuk.org.uk/information-advice/coronavirus/coronavirus-s-guidance/coronavirus-roadmap-lockdown-lifting>. Available from:.
- [41] Institute for Government, Timeline of UK Government Coronavirus Lockdowns and Measures, March 2020 to December 2021, 2021.
- [42] UK Government, COVID-19 response - spring 2021 (Summary). 2021. Accessed; Available from: <https://www.gov.uk/government/publications/covid-19-response-spring-2021/covid-19-response-spring-2021-summary>.
- [43] South Coast Science, Praxis/Urban: Ambient Air Quality Monitor, 2022.
- [44] Alphasense, OPC-N3 Particle Monitor Technical Specification, 2019.
- [45] D. Bousiotis, et al., A study on the performance of low-cost sensors for source apportionment at an urban background site, *Atmos. Meas. Tech.* 15 (13) (2022) 4047–4061, <https://doi.org/10.5194/amt-15-4047-2022>.
- [46] Defra, Site Information for Oxford St Ebbses(UKA00518), 2022.
- [47] Oxford City Council, Oxford High St (OX6), 2022 Available from: https://www.airqualityengland.co.uk/site/latest?site_id=OX6.
- [48] Palas, Fidas® 200 - product lines 2022, Available from: <https://www.palas.de/en/product/fidas200>.
- [49] Defra, Quality Assurance and Quality Control (QA/QC) Procedures for UK Air Quality Monitoring under, 2008. /50/EC and 2004/107/EC. 2013.
- [50] Thermofisher Scientific, 8500 filter dynamics measurement system, Available from: <https://www.thermofisher.com/order/catalog/product/8500>, 2022.
- [51] Defra, UK-AIR: site environment types, Available from: <https://uk-air.defra.gov.uk/networks/site-types>, 2022.
- [52] Z.-M. Zhang, S. Chen, Y.-Z. Liang, Baseline correction using adaptive iteratively reweighted penalized least squares, *Analyst* 135 (5) (2010) 1138–1146, <https://doi.org/10.1039/B922045C>.
- [53] N. Papaioannou, et al., A random forest algorithmic approach to predicting particulate emissions from a highly boosted GDI engine, in: 15th International Conference on Engines & Vehicles, Naples, Italy, September 2021, SAE Technical Paper, 2021, <https://doi.org/10.4271/2021-24-0076>, 2021-24-0076, 2021. SAE International (2021).
- [54] P. deSouza, et al., Calibrating networks of low-cost air quality sensors, *Atmos. Meas. Tech. Discuss.* 2022 (2022) 1–34, <https://doi.org/10.5194/amt-2022-65>.
- [55] F. Pedregosa, et al., Scikit-learn: machine learning in Python, *J. Mach. Learn. Res.* 12 (2011) 2825–2830.
- [56] E. Parliament, Equivalence Spreadsheet Tool on the Demonstration of Equivalence, 2020. Available from: https://ec.europa.eu/environment/air/quality/legislation/pdf/Equivalence_Tool_V3.1_020720.xlsx.
- [57] C.E. Rushton, J.E. Tate, S.P. Shepherd, A novel method for comparing passenger car fleets and identifying high-chance gross emitting vehicles using kerbside remote sensing data, *Sci. Total Environ.* 750 (2021), 142088, <https://doi.org/10.1016/j.scitotenv.2020.142088>.
- [58] Oxford City Council, Oxford City Council Air Quality Action Plan 2021–2025, 2021.
- [59] I. Kloog, et al., Acute and chronic effects of particles on hospital admissions in new-england, *PLoS One* 7 (4) (2012), e34664, <https://doi.org/10.1371/journal.pone.0034664>.